PERGAMON

International Journal of Multiphase Flow 29 (2003) 69–95

International Journal of Multiphase Flow

www.elsevier.com/locate/ijmulflow

Simulation of slug flow in horizontal and nearly horizontal pipes with the two-fluid model

R.I. Issa *, M.H.W. Kempf

Department of Mechanical Engineering, Imperial College of Science, Technology and Medicine, Exhibition Road, London SW7 2BX, UK

Received 26 October 2001; received in revised form 7 October 2002

Abstract

A mechanistic approach to the prediction of hydrodynamic slug initiation, growth and subsequent development into continuous slug flow in pipelines is presented. The approach is based on the numerical solution of the one-dimensional transient two-fluid model equations. The advantage of this approach is that the flow field is allowed to develop naturally from any given initial conditions as part of the transient calculation; the slugs evolve automatically as a product of the computed flow development. The need for the many phenomenological models for flow regime transition, formation of slugs and their dynamics can thus be minimized.

It is shown that when the two-fluid model is invoked within the confines of the conditions under which it is mathematically well-posed, it is capable of capturing the growth of instabilities in stratified flow leading to the generation of slugs. The computed rates of growth of such instabilities compare well with the values obtained from Kelvin–Helmholtz analyses. Simulations are then carried out for a large number of pipe configurations and flow conditions that lead to slug flow. These include horizontal, inclined and V-section pipes. The results of computations for slug characteristics are compared with data obtained from the literature and it is found that the agreement is remarkable given the simplicity of the one-dimensional model.

Keywords: Slug flow; Numerical simulation; Two-fluid model; Growth of instabilities

* Corresponding author. Fax: +44-20-78238845.
E-mail address: r.issa@ic.ac.uk (R.I. Issa).

0301-9322/03/$ - see front matter
PII: S0301-9322(02)00127-1

1. Introduction

Slug flow occurs in many engineering applications such as the transport of hydrocarbon fluids in pipelines, liquid–vapour flow in power plants and buoyancy-driven fermentation equipment (Dukler and Fabre, 1992). It is a highly intermittent flow regime in which large gas bubbles flow alternately with liquid slugs at randomly fluctuating frequency (Fabre and Liné, 1992; Woods et al., 2000). The liquid slugs may be either of pure liquid or are "aerated" as a result of gas entrainment (in the form of small dispersed bubbles) from the large bubbles (Nydal and Andreussi, 1991; Andreussi et al., 1993; Bendiksen et al., 1996). Although the present paper does not deal with the gas entrainment process and the presence of dispersed bubbles in the liquid slug, this is not due to an inherent limitation in the model itself, but is merely for the sake of brevity. The entrainment process can indeed be accounted for within the model as shown by Bonizzi et al. (2001).

In horizontal and nearly horizontal pipes (which are the subject of the paper) slug flow can be generated from stratified flow by two main mechanisms: (i) natural growth of hydrodynamic instabilities and (ii) liquid accumulation due to instantaneous imbalance between pressure and gravitational forces caused by pipe undulations. In the case of the first, small random perturbations of short wavelengths arising naturally, may grow into larger and longer waves on the surface of the liquid (Ansari, 1998). The mechanism behind this growth is the classical Kelvin–Helmholtz (KH) instability (Lin and Hanratty, 1986; Fan et al., 1993a,b). Such waves may continue to grow picking up liquid flowing ahead of them, until they bridge the pipe cross-section, thereby forming slugs. These slugs may grow if the slug fronts travel faster than the tails; conversely they would collapse. Stable slug flow is obtained if the slug front and tail travel at the same speed. In real flow, all these events take place at different times, hence some slugs grow, others collapse; also slugs may travel at different speeds, thereby leading to the merging of some slugs with others (Moissis and Griffith, 1962; Taitel and Barnea, 1990; Zheng et al., 1994).

Slugs may also form at pipe dips due to the retardation and subsequent accumulation of liquid in the dips leading to the filling up of the cross-section with liquid. An extreme example of this terrain induced slug flow is called "severe slugging" and occurs when a slightly inclined pipeline meets a vertical riser (Schmidt et al., 1985; Jansen et al., 1996).

Slug flow may also arise from both of the aforementioned mechanisms simultaneously in long hydrocarbon-transporting pipelines. There, slight terrain undulations may lead to the generation of slugs in addition to those generated by inherent flow instabilities. In such cases, the slugs generated from one mechanism interact with those arising from the second leading to a complex pattern of slugs, which may overtake and combine. Also, slugs undergo changes to their characteristics as they travel through pipe bends and undulations (Taitel and Barnea, 1990; Zheng et al., 1994).

The intermittency of slug flow causes severe unsteady loading on the pipelines carrying the fluids as well as on the receiving devices such as separators. This often gives rise to problems in design and usually leads to design compromises that sacrifice efficiency and/or size of the processing plant. It is therefore important to be able to predict the onset and subsequent development of slug flow; it would be even more desirable if slug characteristics, such as slug length and frequency could be calculated as well. The purpose of the paper is therefore to investigate the capability of the two-fluid model to deliver such predictions in a mechanistic manner and in a unified framework. In particular, the model is shown to be able to simulate the natural growth of instabilities, the formation of successive slugs and the subsequent procession of slug trains. This capability is demonstrated by comparing calculations with experimental data.

Traditional models of slug flow are normally based on the "unit-cell" approach for fully developed slug flow where a control volume encompassing the long gas bubble and the liquid slug is analysed (Wallis, 1969). A steady-state is obtained by selecting a moving frame of reference travelling at the speed of the cell (which is unknown a priori); this enables a steady-state analysis based on mass and momentum balances over the control volume. Many other models based on the "equivalent-unit-cell" concept, and similar approaches were developed (see for example works by Dukler and Hubbard, 1975; Taitel and Barnea, 1990).

Another approach to modelling steady-state slug flow is the statistical averaging of physical properties of the separated and dispersed flow regions. A "statistical cellular model" predicts the dependent variables and the characteristics of the intermittency based on conditional averaging of the conservation equations (Ferschneider, 1983; Fabre et al., 1983; Liné, 1983). Fabre et al. (1992) refined this approach for application to transient flows. Most of the steady-state models are suitable for use in a unified scheme consisting of a general flow pattern prediction model and separate models for the different prevailing flow regimes (see Gomez et al., 1999 for a review). Steady-state models are not able to predict the transition from one flow pattern to another, nor are they necessarily capable of predicting phenomena occurring in inclined pipes, such as the dissipation of slugs in downhill flow as shown by Taitel et al. (2000).

Transient models for slug flow can be classified into categories comprising "empirical slug specification", "slug tracking", and "slug capturing" models.

The empirical slug specification models are used to describe the slug formation, growth, decay, and slug shape (tail and front). These models can be subdivided into "stratified-slug transition", and "slug growth" models. Most methods belonging to the former approach use the classical KH stability theory for inviscid flow (Kordyban and Ranov, 1970; Taitel and Dukler, 1976; Mishima and Ishii, 1986; Lin and Hanratty, 1986; Espedal and Bendiksen, 1989; Watson, 1989). De Henau and Raithby (1995a,b) developed a one-dimensional two-fluid model with a slug flow submodel, which provides the necessary constitutive relations and parameters for the closure relations incorporated in the two-fluid model. Slug growth modelling assumes that a slug has been generated by some mechanism, and correlations are introduced to describe the slug tail and front (Ruder et al., 1989; Jepson, 1989; Lunde and Asheim, 1989; Bendiksen and Espedal, 1992). Bendiksen et al. (1996) incorporated a unit-cell type of slug flow description into the transient two-fluid model. A different modelling approach is presented by Fagundes Netto et al. (1999). They propose a bubble shape calculation based on mass and momentum conservation for bubble body, nose, and tail and for a hydraulic jump at the rear of the bubble.

In slug tracking, the movement, growth and disappearance of slugs are effected by tracking individual slugs. Commonly, slugs are assumed to generate using, say, flow regime maps. Subsequently, the position of each slug tail and front is monitored along the pipe in Lagrangian coordinates with time. This information is then fed into the mass/momentum flux calculations at slug fronts and tails (Bendiksen et al., 1990; Straume et al., 1992). Slug tracking models use, to some degree, empirical correlations to model certain slug properties. An example of the application of such model is in the commercial code OLGA (Bendiksen et al., 1987, 1991). Zheng et al. (1994) suggested a slug tracking technique which predicts growth, generation and dissipation of each slug individually. A similar approach, but applied to the analysis of slug length distribution was proposed by Barnea and Taitel (1993). Nydal and Banerjee (1996) proposed a Lagrangian slug tracking method for dynamic gas–liquid slug flow using an object-oriented approach, whereby slugs and bubbles are treated as discrete computational objects, and organised in linked lists. Taitel and Barnea (1998) proposed another model, which simulates the basic mechanisms of slug generation, growth and dissipation, with particular emphasis on gas compressibility effects.

The method described in the current paper is a slug capturing technique in which the slug flow regime is predicted as a mechanistic and automatic outcome of the growth of hydrodynamic instabilities (Issa and Woodburn, 1998). The stratified, slug and transition regimes are modelled with the same set of governing equations (the one-dimensional, transient, two-fluid model) and closure laws, rendering the use of empirical flow regime models unnecessary. In the simulations, the liquid volume-fraction can increase and eventually becomes unity, thereby leading to the onset of a slug, and this happens naturally as an outcome of the numerical solution of the two-fluid equations. Slugs develop, grow, merge, and collapse depending solely on the solution of the transport equations for mass and momentum for each phase. The only empirical information required is for the closure relations for the liquid–wall, gas–wall and interfacial shear forces (Vernier and Delhaye, 1968; Bouré and Réocreux, 1972; Ishii, 1975; Ishii and Mishima, 1984).

The two-fluid model is well established (Ishii, 1975) and is incorporated in several industrial codes such as PLAC (Black et al., 1990) and OLGA (Bendiksen et al., 1987, 1991). However, it has never been demonstrated conclusively that the model can capture in a natural way the development of slug flow from the growth of instabilities in stratified flow. This is accomplished in the present paper.

2. The two-fluid model

2.1. Governing equations

The basis of the two-fluid model is the formulation of two sets of conservation equations for the balance of mass, momentum and energy for each of the phases. The one-dimensional form of the model is obtained by integrating (area averaging) the flow properties over the cross-sectional area of the flow. The transfer of momentum and energy between the walls and the fluids is included via source terms in the equations and have to be formulated using empirical correlations (Ishii and Mishima, 1984; Jones and Prosperetti, 1985). Furthermore, the dynamic interaction between the phases across the interfaces between them is accounted for by inter-phase forces that appear as source terms in the transport equations. Here again, these are supplied from empirical closure relations. The latter models exert a direct influence in the analysis of flow regime changes that are often attributed to interface instabilities (Ishii, 1975; Drew, 1983; Ishii and Mishima, 1984).

The present study is based on the transport equations for an isothermal flow. Hence the equations solved are for the conservation of mass and momentum for the gas and liquid phases. For one-dimensional stratified and slug flow they are

$$\frac{\partial(\rho_g\alpha_g)}{\partial t} + \frac{\partial(\rho_g\alpha_g u_g)}{\partial x} = -\dot{m}_b, \tag{1}$$

$$\frac{\partial(\rho_l\alpha_l)}{\partial t}+\frac{\partial(\rho_l\alpha_l u_l)}{\partial x}=\dot{m}_b \tag{2}$$

$$\frac{\partial(\rho_g\alpha_g u_g)}{\partial t}+\frac{\partial(\rho_g\alpha_g u_g^2)}{\partial x}=-\alpha_g\frac{\partial p}{\partial x}+\rho_g\alpha_g g\sin\beta+F_{gw}+F_i, \tag{3}$$

$$\frac{\partial(\rho_l\alpha_l u_l)}{\partial t}+\frac{\partial(\rho_l\alpha_l u_l^2)}{\partial x}=-\alpha_l\frac{\partial p}{\partial x}-\rho_l\alpha_l g\frac{\partial h}{\partial x}\cos\beta+\rho_l\alpha_l g\sin\beta+F_{lw}-F_i, \tag{4}$$

where

$$\alpha_g+\alpha_l=1. \tag{5}$$

The subscripts g, l, and i refer to the gas and liquid phases, and the interface, respectively. The axial coordinate is x, the density is ρ, the phase fraction is α, the velocity is u, the mass transfer per unit volume between the phases is $\dot{m}_b$, the interface (and gas) pressure is p, the pipe inclination is β, the height of the liquid surface (assumed flat) above the pipe bottom is h and the acceleration due to gravity is g. The liquid is assumed to be incompressible, while the gas is taken to be compressible obeying the ideal-gas equation of state; the flow is assumed to be isothermal for the sake of simplicity, but the assumption is not a necessary requisite to the model. The second term on the right hand side of Eq. (4) relates to the hydrostatic pressure in the liquid and is specific to the stratified and slug flow regimes that are the subject of interest here. The terms F, stand for the frictional forces per unit volume between each phase and the wall, and between the phases themselves (at the interface). These terms need closure models and are the subject of investigation in Section 2.2.

2.2. Closure models

2.2.1. Specific models

The closure relations needed in the two-fluid model are for the liquid–wall, gas–wall and interfacial shear forces. The most common models are based on the prescription of a friction factor, where the shear stress τ for one-dimensional flow is given by:

$$\tau=\tfrac{1}{2}f\rho|u_r|u_r. \tag{6}$$

The term u_r stands for the relative velocity between either the liquid and the wall, the gas and the wall, or the liquid and the gas. The liquid density is used in Eq. (6), when the shear stress at the liquid–wall contact is determined; for the gas–wall and liquid–gas interfaces the density of the gas phase is used. In this work, several formulations for the friction factor f have been implemented and evaluated. Those were due to: Manning (dating back to 1864, see e.g. Wallis, 1969) Taitel and Dukler (1976), Andritsos and Hanratty (1987), Kowalski (1987), Hand (1991), Srichai (1994), Grolman and Fortuin (1996). In the evaluation, the criteria for an optimum combination of liquid–wall, gas–wall, and interfacial friction factors were taken as: (i) correct prediction of flow regime transition boundaries; (ii) good prediction of slug characteristics, e.g. slug frequency and translational velocity; (iii) reasonable range of discrepancy with data over all flow conditions.

The Manning relationship is derived from open channel flow and adapted to multiphase flow. Taitel and Dukler (1976) proposed a similar expression to the relationship by Blasius (e.g.

Agrawal et al., 1973), with modified coefficients based on experimental evidence. Andritsos and Hanratty (1987) developed an expression for a wavy interfacial friction. Kowalski (1987) proposed a friction factor for the liquid–wall interface based on measurements of stratified flow, and an interfacial friction factor based on indirect determination from a momentum balance. Hand (1991) proposed a friction factor relationship based on stratified flow data in air–water flow. Srichai (1994) gives an expression for a liquid–wall friction factor based on stratified flow data. Grolman and Fortuin (1996) present the so-called modified apparent rough surface (MARS) model, in which the friction factor relationships are functions of each other.

2.2.2. Comparison of models

The results of continuing work that culminates in this paper indicate little sensitivity to the gas–wall friction model. As most works in the literature agree that the Taitel and Dukler (1976) relationship for this force to be the most accurate, this model has therefore been adopted for the frictional force between the gas and the wall in all computations presented herein.

For the interfacial friction factor, Kowalski's relationship was found to induce flow instability too readily, particularly at the pipe inlet. Hand's, and Andritsos and Hanratty's relationships for a wavy interface tended to increase the average liquid velocities, hence leading to earlier attainment of the critical slug formation velocity. The slug frequency and the global hold-up were found to reduce, resulting in a slight underprediction of the experimental data. Here again, the Taitel and Dukler (1976) relationship was found to be best and was adopted.

In a study leading to this paper, it was found that the onset and growth of instabilities resulting in slugging, was most sensitive to the model used to represent the wall friction force on the liquid phase, but was hardly affected by the interfacial and gas–wall forces. The liquid–wall friction factor relationship of Manning failed to give slugs even at high flow rates. Its value is independent of the liquid flow rate, and at a value significantly different from those predicted by other relationships. It therefore could not account for the dynamic changes in the velocities of the two phases and as a consequence never yielded the liquid velocity required to initiate slug formation. These results are perhaps not surprising since the Manning formula was originally derived for open channel flow, a configuration quite different from that of two phase flow. The Taitel and Dukler (1976) relationship was reasonably successful in predicting the correct flow regime transition boundary given in the well-known Taitel and Dukler flow regime map. The model was most successful for lower gas flow rates in the slug regime. At higher gas flow rates, however the computational slug frequencies and translational velocities differ significantly from experimental data. The model of Kowalski (1987) for the liquid–wall friction factor showed reasonable results with good transition to the slug flow regime for low flow rates. However, it failed to predict slug flow at higher flow rates. Similar to the Kowalski model, Srichai's model gives good predictions at low flow rates, but the accuracy decreases significantly at higher ones. Srichai simply modified the coefficients in the Kowalski expression to fit his own data, which might be the reason for the similarity in the results of the two models. Hand (1991) modified Kowalski's relationship, and this proved to be more successful than Kowalski's and Srichai's models in the present computations. The correlation of the computational and experimental slug properties give approximately constant differences over all flow rates, with an error bound of around $\pm 20\%$. The MARS model by Grolman and Fortuin (1996) did not predict slugging at all, and subsequently was discarded from further analysis.

Subject to the criteria given earlier, and after extensive evaluation of all the models presented above, the final selection of the models that gave the best results was made; these are as follows. For the gas–wall, and interfacial friction factors, either the well known Hagen–Poiseulle formula:

$$f_g = \frac{16}{Re_g}, \quad f_i = \frac{16}{Re_i}, \tag{7}$$

is used in laminar flow or the Taitel and Dukler (1976) correlation:

$$f_g = 0.046(Re_g)^{-0.2}, \quad f_i = 0.046(Re_i)^{-0.2}, \tag{8}$$

is invoked for turbulent flow, respectively. For the liquid phase shear stress the friction factor by Hand (1991), and Spedding and Hand (1997) is used. The correlation is given by:

$$f_l = \frac{24}{Re_l} \tag{9}$$

for laminar flow, and

$$f_l = 0.0262(\alpha_l Re_l)^{-0.139} \tag{10}$$

for turbulent flow. In the above equations α_l is the volumetric liquid hold-up, and the Reynolds numbers Re_g, Re_i and Re_l are taken as:

$$\begin{aligned} Re_g &= \frac{4A_g u_g \rho_g}{(S_g + S_i)\mu_g}, \\ Re_i &= \frac{4A_g |u_g - u_l| \rho_g}{(S_g + S_i)\mu_g}, \\ Re_l &= \frac{DU_{sl}\rho_l}{\mu_l}, \end{aligned} \tag{11}$$

respectively. The density is ρ, the dynamic viscosity is μ and the superficial liquid velocity is U_{sl}. For a pipe with cross-section A and diameter D, the area occupied by the gas and the liquid is A_g and A_l, respectively, the wetted perimeter of the gas and the liquid is S_g and S_l, respectively, and the interfacial width is S_i, as shown in Fig. 1.

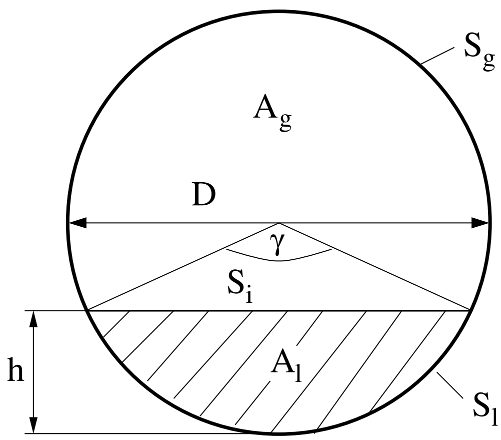

Fig. 1. Pipe cross-section.

It should be noted that the interface Reynolds number Re_i is based on the gas density and the slip velocity between the liquid and gas; this is a standard practice.

All the results for slug flow that are presented in what follows, are computed using the above combination of closure models.

2.3. Numerical solution

The transport equations (1)–(4) are solved numerically (Issa and Abrishami, 1986). They are first discretised on a staggered grid using a finite volume method. On a staggered grid, the velocities are stored at locations midway between pressure nodes to avoid the decoupling of velocity and pressure. Fig. 2 shows a staggered grid arrangement for the one-dimensional domain, with control volumes given for pressure and velocity cells. The symbol p refers to the centres of the control volumes (whether continuity or momentum), and E and W refer to the neighbouring nodes. Symbols e and w denote cell face values for the control volume surrounding node p. The finite volume formulation of the continuity equation for time step $k+1$ for either the gas or the liquid phase is given by:

$$\frac{\delta x_p}{\delta t}(\rho_p^{k+1}\alpha_p^{k+1} - \rho_p^k\alpha_p^k) + (\rho_e u_e - \rho_w u_w)^{k+1}\alpha_p^{k+1} + (\max(\rho_w u_w, 0)^{k+1} - \min(\rho_e u_e, 0)^{k+1})\alpha_p^{k+1}$$
$$+ (\min(\rho_e u_e, 0)^{k+1})\alpha_e^{k+1} - (\max(\rho_w u_w, 0)^{k+1})\alpha_w^{k+1} = 0,$$

where the upwind difference scheme is invoked for the spatial derivatives and the Euler implicit scheme is used for temporal integration. Similarly, the discretized momentum equation for either the gas or the liquid is given by:

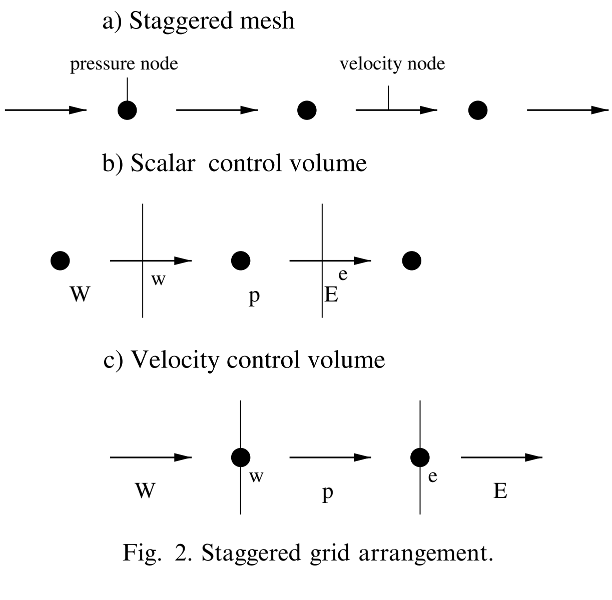

Fig. 2. Staggered grid arrangement.

$$\frac{\delta x_p}{\delta t}(\rho_p^{k+1}\alpha_p^{k+1}u_p^{k+1} - \rho_p^k\alpha_p^k u_p^k) + (\alpha_e\rho_e u_e - \alpha_w\rho_w u_w)^{k+1}u_p^{k+1}$$
$$+ (\max(\alpha_w\rho_w u_w, 0)^{k+1} - \min(\alpha_e\rho_e u_e, 0)^{k+1})u_p^{k+1} + (\min(\alpha_e\rho_e u_e, 0)^{k+1})u_e^{k+1}$$
$$- (\max(\alpha_w\rho_w u_w, 0)^{k+1})u_w^{k+1} + \alpha_p^{k+1}(p_e - p_w)^{k+1} - \Phi = 0, \tag{13}$$

where again the upwind difference and Euler implicit schemes are employed. The source term Φ takes different forms in the liquid and gas momentum equations. For the gas phase it is:

$$\Phi_g = \frac{1}{2A}(-f_{g,p}\rho_{g,p}u_{g,p}S_{g,p} - f_{i,p}\rho_{g,p}|u_{l,p} - u_{g,p}|S_{i,p})^{k+1}u_{g,p}^{k+1}\,\delta x_p$$
$$+ \frac{1}{2A}(f_{i,p}\rho_{g,p}|u_{l,p} - u_{g,p}|S_{i,p})^{k+1}u_{l,p}^{k+1}\,\delta x_p + \alpha_{p,g}^{k+1}\rho_{p,g}^{k+1}g\,\delta x_p\sin\beta, \tag{14}$$

while for the liquid phase it is:

$$\Phi_l = \frac{1}{2A}(-f_{l,p}\rho_{l,p}u_{l,p}S_{l,p} - f_{i,p}\rho_{g,p}|\mu_{l,p} - \mu_{g,p}|S_{i,p})^{k+1}u_{l,p}^{k+1}\,\delta x_p$$
$$+ \frac{1}{2A}(f_{i,p}\rho_{g,p}|u_{l,p} - u_{g,p}|S_{i,p})^{k+1}u_{g,p}^{k+1}\,\delta x_p + \alpha_{p,l}^{k+1}\rho_{p,l}^{k+1}g(h_e - h_w) + \alpha_{p,l}^{k+1}\rho_{p,l}^{k+1}g\,\delta x_p\sin\beta. \tag{15}$$

When a slug forms, the liquid phase fraction reaches unity and that of the gas phase tends to zero. This results in the gas momentum equation becoming singular since the gas phase fraction multiplies both sides of the equation. In order to prevent spurious numerical values for the gas velocity resulting from solving a singular equation within the regions occupied by liquid alone, the gas phase momentum equation is suppressed in that region and the gas velocity is arbitrarily set to zero (that value is immaterial since the region contains only liquid). Everywhere else, the two-fluid model equations are solved in full.

A pressure equation is derived by combining the two continuity equation (12) together with the momentum equation (13) to obtain:

$$\hat{\alpha}_{l,E}^{k+1}u_{l,E}^{k+1} - \hat{\alpha}_{l,W}^{k+1}u_{l,W}^{k+1} + \frac{1}{\rho_{g_{ref}}}(\hat{\alpha}_{g,E}\hat{\rho}_{g,E}u_{g,E} - \hat{\alpha}_{g,W}\hat{\rho}_{g,W}u_{g,W})^{k+1} + \frac{\delta x_p}{\delta t}(\alpha_{l,p}^{k+1} - \alpha_{l,p}^k)$$
$$+ \frac{1}{\rho_{g_{ref}}}\frac{\delta x_p}{\delta t}(\alpha_{g,p}^{k+1}\rho_{g,p}^{k+1} - \alpha_{g,p}^k\rho_{g,p}^k) = 0, \tag{16}$$

where $\hat{\alpha}$ denotes upwinded values of the phase fraction (corresponding to the upwind values appearing in the parent equations). It should be noted that the gas and liquid phase equations are volume-weighted (by division by the constant liquid density and a reference gas density $\rho_{g_{ref}}$, respectively) before being combined. Otherwise the pressure equation may become dominated by terms relating to the heavier liquid phase thereby leading to convergence problems.

The resulting set of equations comprising: momentum equation (13), the pressure equation (16), and an equation for the volume fraction (taken to be the continuity equation (12) for the gas) are solved sequentially in an iterative manner at each time step until convergence. The numerical procedure is embodied in a computer code called TRIOMPH.

The boundary conditions used in all the calculations are as follows. At the pipe inlet, the liquid and gas flow rates and volume fractions were specified and were assumed to remain steady at those values. The pressure at the pipe outlet was fixed at its standard atmospheric value.

Accuracy of the solution was verified by successive grid refinement until the solution was found to be independent (statistically where appropriate) of the number of nodes. The computations presented herein were carried out keeping the dimensionless number $(\delta t/\delta x)u^k_{g_{max}}$ constant at 0.5 which implies that as the mesh is refined, the time step size is correspondingly reduced. It is worth noting that the time steps used correspond to Courant numbers (for a compressible flow computation) between 10 and 20. In this paper, only results of mesh refinement studies are presented. Studies on the effect of the size of the time step while keeping the mesh spacing fixed were carried out by Woodburn and Issa (1998) who found that the time step had no effect on the solution for values of $(\delta t/\delta x)u^k_{g_{max}}$ around unity.

3. Growth of instabilities and well-posed equations

One-dimensional, unsteady two-phase flow codes employing the two-fluid model are frequently relied upon in the oil and nuclear industries to simulate transient phenomena which occur in ducts and pipelines either as a result of controlled changes in flow conditions or from accidents. They are however seldom utilized to predict the onset of slugging or subsequent slug flow development. Indeed, such calculations are treated with suspicion as being spurious. This is because the two-fluid equations governing the flow are known to be ill-posed mathematically under certain conditions depending on the closure models incorporated to represent inter-phase forces (Wallis, 1969; Stuhmiller, 1977; Jones and Prosperetti, 1985; Barnea and Taitel, 1994). However, the ill-posedness of the basic governing equations seldom manifests itself clearly in the numerical solution and therefore goes undetected. This uncertainty is further compounded by the association in some of the literature of the switch from ill to well posedness of the equations (which occurs as the flow conditions change) with the onset of actual flow instabilities. Hence, computations beyond the onset of instability are usually discarded. This confusion has been addressed by Woodburn and Issa (1998) who demonstrated that flow instabilities can be captured by numerical simulations when the equation system is well-posed. This aspect is reiterated in the present paper.

Flow stability is a property of the fluid dynamics of the flow. It refers to the tendency of the flow to return to its original state after being perturbed. The growth or decay of perturbations is determined by the fluid dynamics of the flow rather than the modelling process, though the accuracy of the models can significantly affect the stability of the simulated flow and the computed growth rate of waves and perturbations. Commonly, the stability of the flow is investigated by a linear perturbation analysis of the governing equations. The resulting dispersion equation which gives the magnitude of a perturbation as a function of space and time is satisfied by an exponential solution:

$$\Psi = \Psi_0 e^{i(\omega t - kx)}, \tag{17}$$

which also directly indicates whether the flow is stable or not (Jones and Prosperetti, 1985; Lin and Hanratty, 1986; Brauner and Maron, 1992). In Eq. (17), Ψ stands either for the pressure p, the density ρ, the velocity u, or the phase fraction α. The amplitude of the original perturbation is Ψ_0, the complex wavenumber is k, and the complex frequency is ω; the growth rate of the perturbation is given by the negative imaginary part of the complex frequency, and is denoted as $-\omega_i$.

Barnea and Taitel (1994) used a linear KH analysis to study the onset of instability for both inviscid (IKH) and viscous (VKH) flow, using the two-fluid model. The criteria they found are:

$$(u_g - u_l) < K\sqrt{(\rho_l\alpha_g + \rho_g\alpha_l)\frac{\rho_l - \rho_g}{\rho_l\rho_g}g\cos\beta\frac{A}{\frac{dA_l}{dh}}}, \tag{18}$$

where for the inviscid case the factor $K = 1$, and for the viscous case:

$$K = \sqrt{1 - \frac{(C_v - C_{iv})^2}{\frac{\rho_l-\rho_g}{(\rho_l/\alpha_l)-(\rho_g/\alpha_g)}g\cos\beta\frac{A}{dA_l/dh}}}, \tag{19}$$

and where the pipe cross-sectional area is A, and the cross-sectional area occupied by the liquid is A_l. The critical wave velocities from the inviscid and viscous stability analyses are C_{iv} and C_v, respectively (Barnea and Taitel, 1994). It can be shown that the velocities at which IKH instabilities initiate are higher than those at which VKH instabilities are triggered.

Well-posedness is a property of the modelling process, rather than a specific property of the flow itself and requires that the model appropriately reflects the physics of the flow. A necessary condition for an initial-value problem to be well-posed is that the governing differential equations should possess real characteristics (see for example Garabedian, 1964; Anderson, 1995; Song and Ishii, 2000). For incompressible flow the two-fluid model has been shown to possess real characteristics when the relative velocity between the two phases falls below a certain value. This value coincides with the IKH stability criterion defined by Eq. (18) with $K = 1$. A recent analysis (Bonizzi, 2002) of the characteristics of the two-fluid model equations but with a compressible gas phase (as the set solved here) revealed that the limiting criterion for obtaining real characteristics is the same as that when both phases are incompressible.

It is not immediately obvious whether instabilities predicted by the two-fluid model are legitimate solutions that actually reflect real flow instabilities or whether they are manifestations of mathematical/numerical instability. There exist three different flow regimes with different properties of well-posedness and stability (Barnea, 1991; Barnea and Taitel, 1994). Relative velocities above IKH limit (Taitel and Dukler, 1976; Mishima and Ishii, 1986) lead to an ill-posed system with imaginary characteristics. A system with relative velocities between the IKH and VKH limits (Wallis, 1969; Lin and Hanratty, 1986; Barnea, 1991) results in real characteristics, and is hence well-posed. However, the flow itself is unstable according to the criteria in Eqs. (18) and (19) established by the usual linear stability analysis. A system with velocities below the VKH limit is well-posed and describes stable flow. All of the above was demonstrated by Woodburn and Issa (1998).

The configuration studied here is that of a uniform area horizontal pipe (like that studied by Woodburn and Issa, 1998), into which water and air flow in a stratified state; it is depicted in Fig. 3. For this study both phases are assumed to be incompressible (unlike the rest of the results to be presented later where the gas compressibility is taken into account). Small perturbations are introduced in the form of a continuous sine wave in phase fraction (keeping the superficial velocities constant) at inlet, with a period of 1 s. The growth (or decay) of the perturbations is monitored in time and the rate of such growth is determined by plotting the amplitude of the disturbance as it propagates into the pipe, against time. The growth rate can then be compared against the analytic value obtained from the KH stability analysis. The grid was refined successively in order to diminish the numerical errors and converge to an accurately resolved solution; this test should also reveal whether the system of equations is well-posed or not, in that if the solutions converge to the same result with grid refinement, then the model is sound.

The results shown in Fig. 4 correspond to flow conditions of an inviscid flow with a relative phase velocity of 20 m/s and an IKH limit (critical velocity) of 14.09 m/s. At this supercritical velocity the system of equations is ill-posed, as no real characteristics exist. The figure depicts hold-up profiles at some instant in time along the pipe predicted with different mesh densities given as mesh spacing per "reference" wave length (in the absence of prior knowledge of the actual wavelength generated this reference wavelength is determined as the length of a wave that would travel at the same velocity as the liquid). For this case, the solution continues to change with mesh refinement with the different solutions departing further and further from each other as the mesh is refined. This is amply reinforced in Fig. 5 where computed values of the growth rate of the disturbance are plotted for the different mesh sizes. The figure clearly shows that the wave

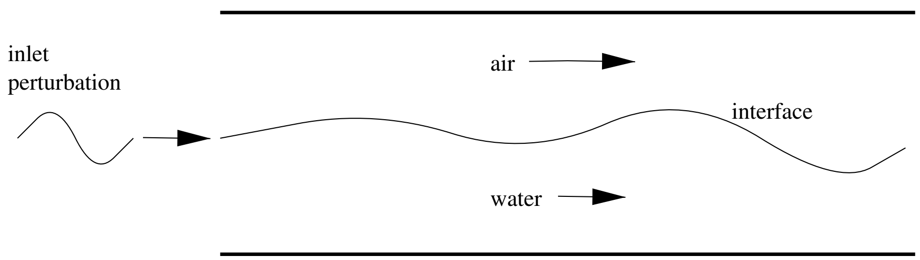

Fig. 3. Perturbation of interface in two-phase pipe flow.

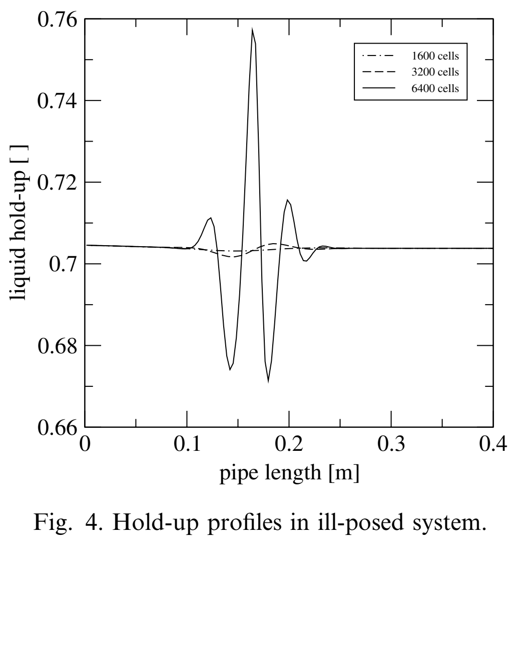

Fig. 4. Hold-up profiles in ill-posed system.

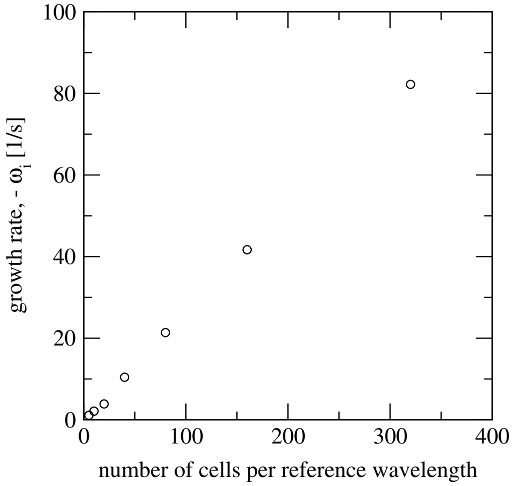

Fig. 5. Growth rate in ill-posed system.

growth rate increases indefinitely with mesh refinement and would never converge onto a unique solution. Indeed its value tends rapidly towards infinity as other computations, not shown here, have revealed. This behaviour is taken to be a sign of the ill-posedness of the equations being solved.

In contrast, a supercritical flow with a relative phase velocity of 12.5 m/s (between the IKH limit of 14.09 m/s, and the VKH limit of 4.75 m/s) leads to a well-posed system, and successive solutions tend to the same result, as shown in Fig. 6 which depicts hold-up profiles at some instant in time along the pipe for different mesh densities. It should be pointed out that in the figure, the differences between the solutions are somewhat exaggerated by the scale of the plot which is necessitated by the desire to show the waves clearly. The case considered here corresponds to one

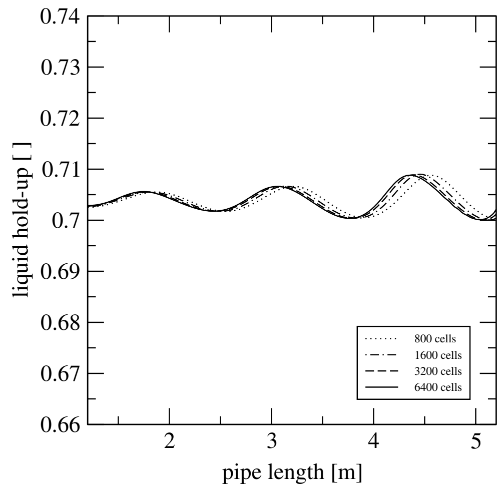

Fig. 6. Hold-up profiles in well-posed system.

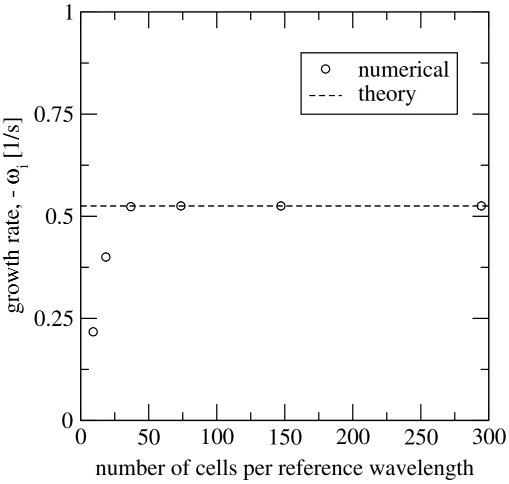

Fig. 7. Growth rate in well-posed system.

of supercritical flow where the flow instability should grow as is indeed predicted. In Fig. 7 the predicted growth rate (ω_i in Eq. (17)) is plotted as a function of the number of grid nodes per wavelength and is compared with the linear theoretical growth rate (dashed line in the figure) using the stability analysis of Barnea and Taitel (1994). The numerical solution clearly tends to an asymptotic value (signifying convergence to a single solution unlike in the previous ill-posed case) and this is taken as being evidence that the system of equations is well-posed for the given flow conditions, even though the flow itself is unstable. This value for growth rate agrees excellently with the analytical value even though the latter is based on a linear analysis while the numerically predicted value is obtained from a fully non-linear model.

It should be emphasized, that if flow instabilities are to be captured, the numerical solution must be sufficiently accurate and relatively free of discretisation errors. This was achieved in this study by high mesh densities. Otherwise, numerical errors (numerical diffusion in particular) can suppress these instabilities and prevent them from growing. They can also mask the ill-posed nature of the system of equations being solved by the introduction of high artificial diffusion, thereby damping out numerical (rather then real flow) instabilities.

4. Slug initiation, growth and development

4.1. Preamble

This section presents the results of calculations for slug flow using the two-fluid model described earlier. The aim of the computations is to verify that the model is capable of predicting the initiation and subsequent growth and development of slugs in an automatic manner starting from steady stratified-flow as an initial state. It is emphasised that in all calculations, slugging initiates automatically and no perturbations need to be introduced artificially to induce it. Such perturbation is bound to arise naturally, from numerical truncation, machine round-off in the computations or starting from non-equilibrium flow. It should however be remarked that when compressibility of the gas is included in the calculations, slugs generate more readily and (as will be shown later when the results are compared with measurements) at the right frequency. On the other hand, if both fluids are treated as incompressible, slugging can still develop, but more slowly and at a lower frequency than what the data indicate. Hence, it is important to account for gas compressibility for accurate prediction of slug characteristics. This is not surprising, since the predicted temporal and spatial variations in pressure (and hence density) when slugs are formed can be as high as 40% thus making gas compressibility effects a significant factor.

In producing the results presented below, care was taken to ensure that the solutions are numerically resolved by carrying out systematic mesh refinement regularly. Furthermore, local checks were made during the calculations to verify that the system of equations being solved was predominantly well-posed for those flow conditions. This could easily be done using Eqs. (18) and (19) to check the nature of the system at each mesh point. Solutions where the equation system was persistently ill-posed, were discarded. In general it was found that within the slug regime itself, the model equations are usually well-posed (in the slug body the flow is that of a single phase and condition (18) ceases to apply).

In what follows, three pipe configurations were studied: a horizontal pipe, a downward inclined pipe and a V-section (see Fig. 8). The predictions are compared with various experimental data for

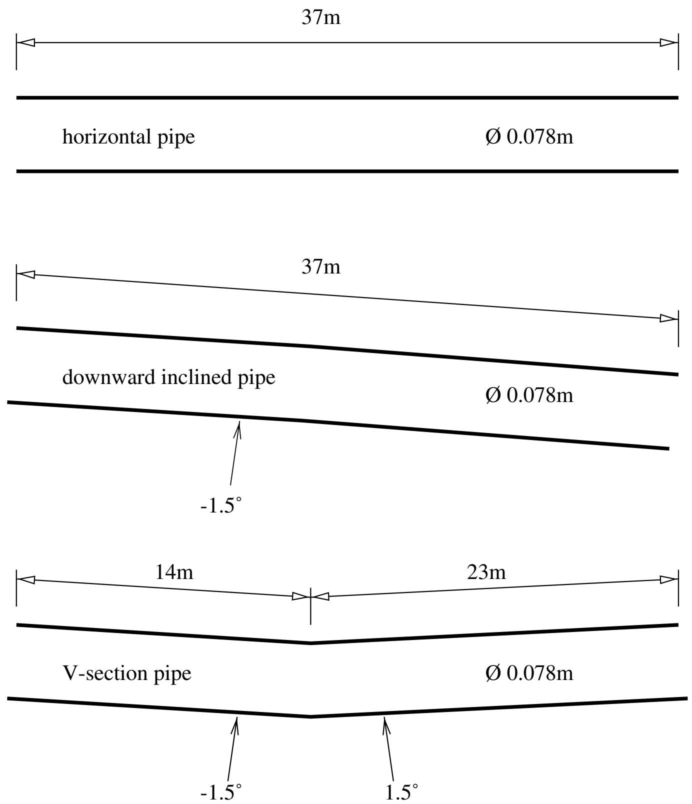

Fig. 8. Horizontal, downward inclined, V-section pipes.

air–water systems, which are obtained from the WASP facility at the Chemical Engineering department of Imperial College (conducted by Hewitt and co-workers), as well as ones gathered from the published literature. The first two cases (horizontal and inclined pipes) are examples in which hydrodynamically induced slugging takes place. The third case (V-section) is one where slugs initiate due to both terrain undulations and hydrodynamic instability. The results presented herein, comprise flow regime maps, slug frequencies, slug translational velocities, mean hold-up, and average slug body length. The predictions show remarkably good agreement with the data considering the complexity of the slug flow regime and the simplicity of the one-dimensional model.

In all computations, the initial liquid hold-up, gas velocity and liquid velocity were taken as uniform along the pipe (corresponding to stratified flow). The computational mesh is made up of 1250 cells for all three cases; this was found (through mesh refinement) to give acceptably accurate solutions.

4.2. Horizontal and downward inclined pipe

The pipe used is 36 m long and has an internal diameter of 0.078 m, as in the experiment. The downward inclined pipe slopes at an angle of 1.5° to the horizontal. The effect of small pipe inclinations on the transition to slug flow is treated in several articles (e.g. Barnea et al., 1980; Andreussi and Persen, 1987; Stanislav et al., 1986; Grolman et al., 1996; Taitel et al., 2000; Woods et al., 2000). Most of these authors found that higher liquid flow rates are necessary to obtain slugs in downflows, and vice versa for upflows. Furthermore, slugs can dissipate faster in downhill sections, than in horizontal ones.

Fig. 9 shows typical predicted liquid phase fraction distributions in slug flow in a horizontal pipe at different instants in time. For clarity of presentation, the different curves are shifted relative to each other with respect to time. The superficial gas and liquid velocity are 2 and 1 m/s, respectively. The trace clearly shows the time evolution of growing disturbances in stratified flow, leading to continuous slugging of the pipe (when the liquid phase fraction goes to one). The onset of this hydrodynamic slugging occurs about 7 m from the pipe inlet, and 7 s after the start of the computation from uniform stratified flow initial conditions.

Many such computations were carried out for different combinations of the liquid and gas velocities, to establish the conditions under which slugging initiates. The flow pattern maps predicted by the computations are shown for horizontal and downward inclined pipes in Figs. 10 and 11, respectively.

Fig. 10 shows the predicted flow regime type (shown as points) on a flow regime map in comparison to the Taitel and Dukler (1976) transition lines for horizontal flow. The region of stratified-wavy flow as defined by Taitel and Dukler, is one which is difficult to reproduce exactly in the present one-dimensional computations. This is because, in the simulations, only reasonably long waves generated by KH type of instabilities could be captured, whereas the surface waves in reality include shorter waves, which may not be accounted for in the present one-dimensional model. Nonetheless, computations where waves were continuously generated, but which did not lead to slugging are classified herein as representing "stratified-wavy" flow; this may be debatable. Nevertheless, the comparison with the Taitel and Dukler transitions lines shows that the model is

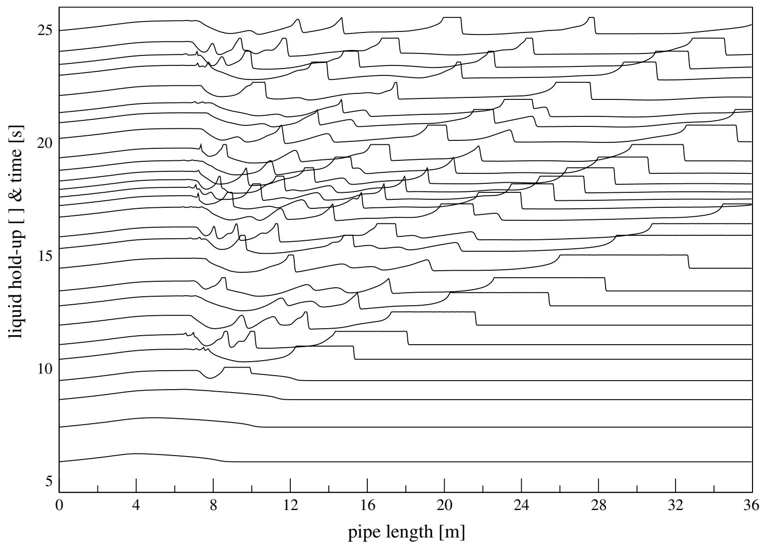

Fig. 9. Typical time trace hold-up in slug flow.

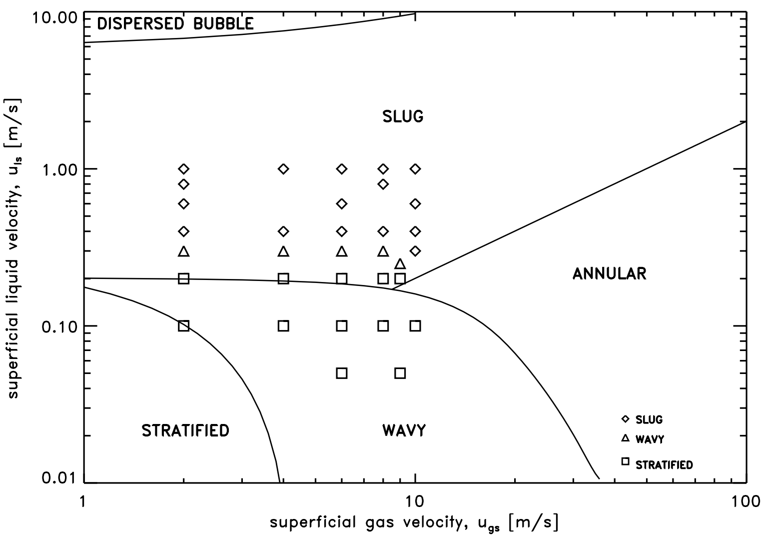

Fig. 10. Flow pattern map, horizontal configuration.

indeed capable of predicting the transition from stratified to slug flow with a fair degree of accuracy, and this is achieved in a natural manner.

Fig. 11 presents the predicted flow regimes for the downward inclined pipe. The transition lines shown in the figure are those obtained experimentally (Manolis et al., 1995a; Manolis, 1995). Here again, the computational points designated as belonging to the stratified wavy regime are ones where the predicted flow exhibited continually-generated waves that did not bridge the pipe to

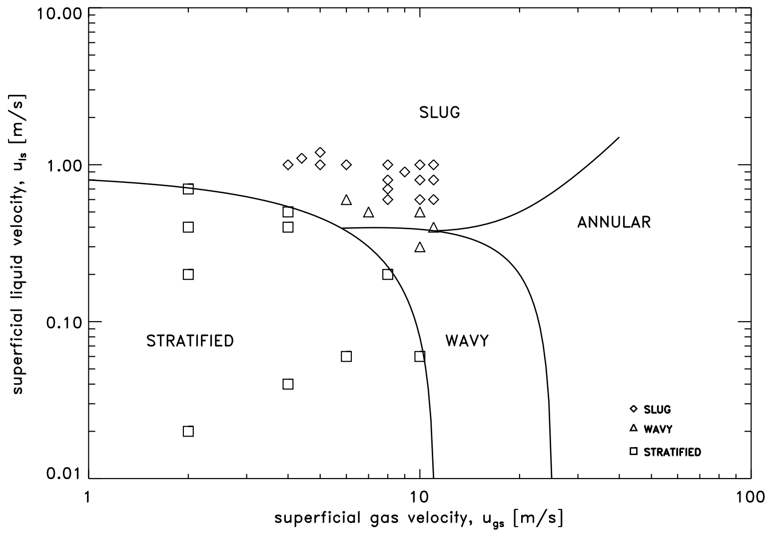

Fig. 11. Flow pattern map, downward inclined configuration.

form slugs. It should be remarked that beyond a value of gas superficial velocity of around 11 m/s, the model becomes ill-posed, and the numerical solutions that were obtained were discarded in accordance with the conclusions reached earlier regarding the validity of such solutions. Hence, not many results can be presented within the region defined as stratified-wavy in the experiments. Overall, the comparison between the computations and experiment is very good, with transition from stratified to slug flow being predicted well below gas superficial velocities of 10 m/s.

It should be noted that the predicted slugs exhibit a similar trend to those in real slug flow in that they are not all of the same length or frequency. Indeed there is an element of statistical randomness in their characteristics as is the case in actual flow. A typical histogram of the slug lengths produced is shown in Fig. 12 as an example. Such a histogram is obtained from the computations by monitoring the liquid hold-up at two points along the pipe (near the outlet) in time. From these hold-up values the times of arrival and departure of slugs are established and from these, the slug translational velocity can be determined. The length of each slug that passes can thus be calculated from the passage time and the slug velocity (in much the same way as is done in actual experiments). The computed values shown in the figure relate to a case with gas and liquid superficial velocities of 4 and 0.4 m/s, respectively. The experimental evidence for this case indicate that the slug lengths are typically in the range of 12–30 times the pipe diameter (Dukler and Hubbard, 1975; Dukler et al., 1985; Nydal et al., 1992). Also as in real slug flow, the variations in slug characteristics occur around a statistical mean, which is what is used to compare the calculations against the data in what follows.

Fig. 13 compares computed and experimental slug frequencies; the experimental data are by Manolis et al. (1995b) and Manolis (1995). The majority of the computed points are within a 20% bound, which is typical for experimental scatter. The numerical solutions underpredict the frequencies for horizontal flow, but overpredict them for downward flow, although the discrepancy for the latter is only around 5%. Figs. 14 and 15 show the computational frequencies in com-

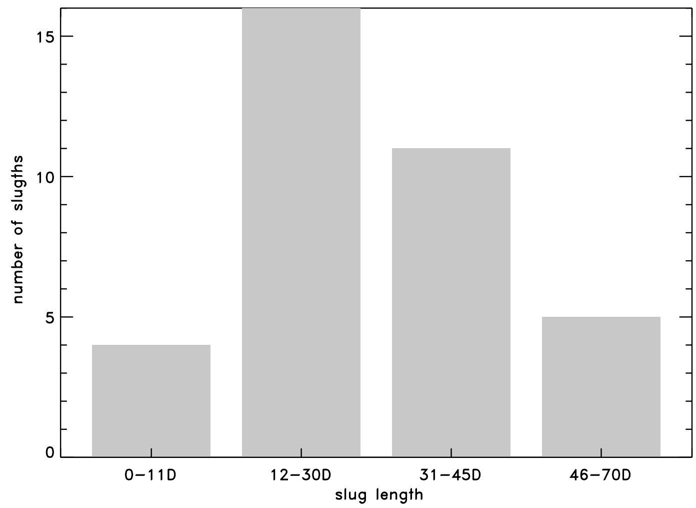

Fig. 12. Typical slug length histogram.

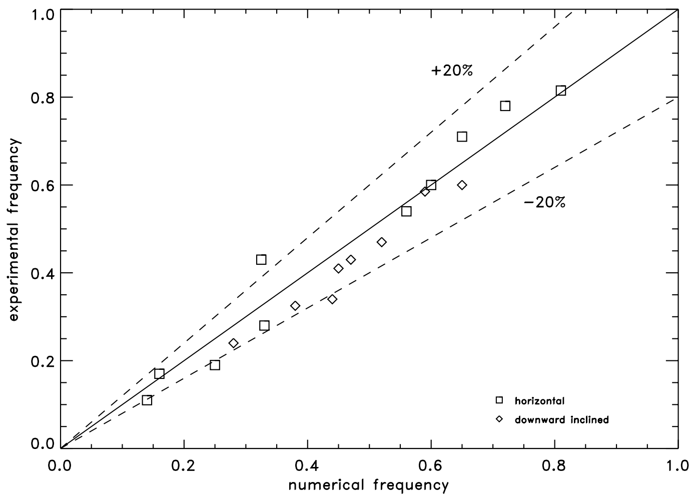

Fig. 13. Slug frequencies in horizontal and downward pipes.

parison to the empirical correlation of Gregory and Scott (1969) who give an expression for the frequency ϕ as:

$$\phi = 0.0226\left(\frac{u_{\mathrm{ls}}}{gD}\left(\frac{19.75}{u_{\mathrm{m}}} + u_{\mathrm{m}}\right)\right)^{1.2}, \tag{20}$$

where the superficial liquid velocity is u_{sl}, the gravitational constant is g, and the mixture velocity is u_{m}. The computational frequencies show good agreement with the correlation, with discrepancies typically around 10%. The translational slug velocities are shown in Fig. 16. The straight

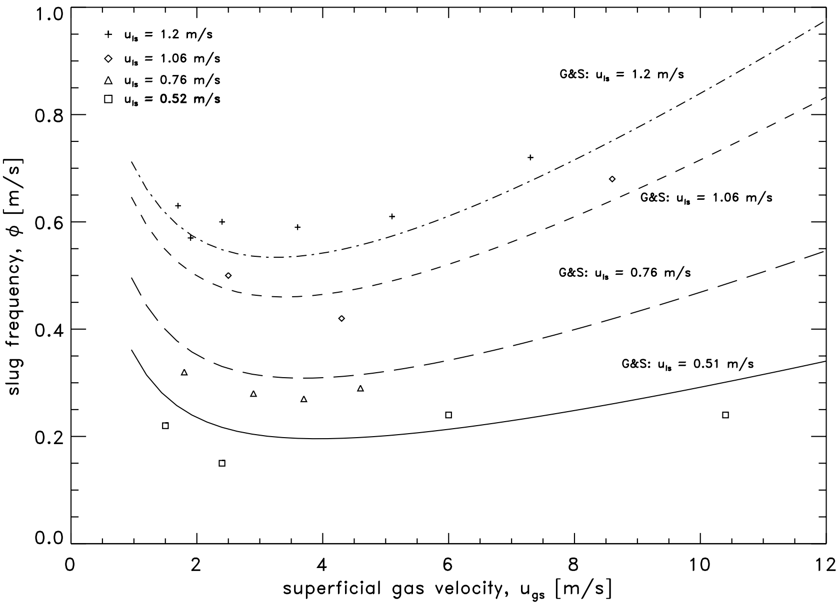

Fig. 14. Slug frequencies in horizontal pipe.

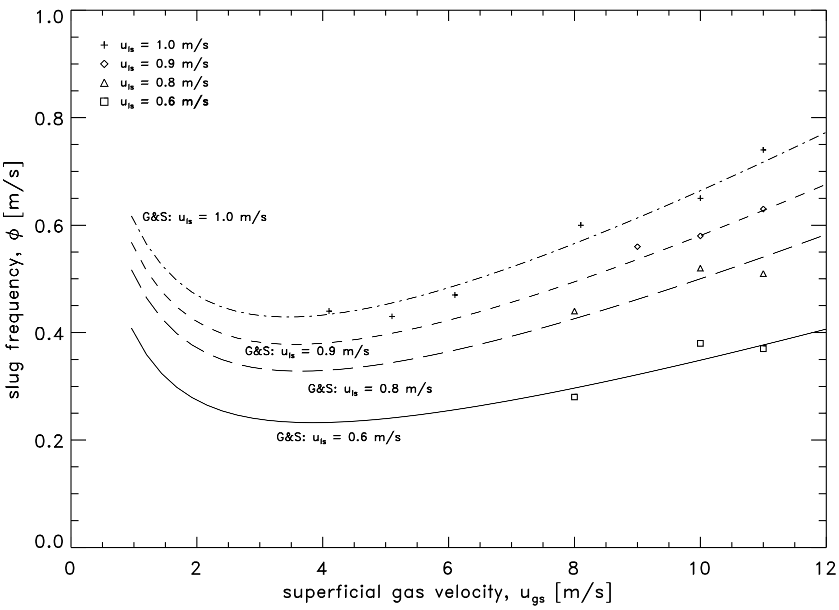

Fig. 15. Slug frequencies in downward pipe.

line in the figure corresponds to a translational velocity of 1.2 times the mixture velocity, which is a commonly used empirical correlation. The agreement between the present calculations and this correlation is fairly good.

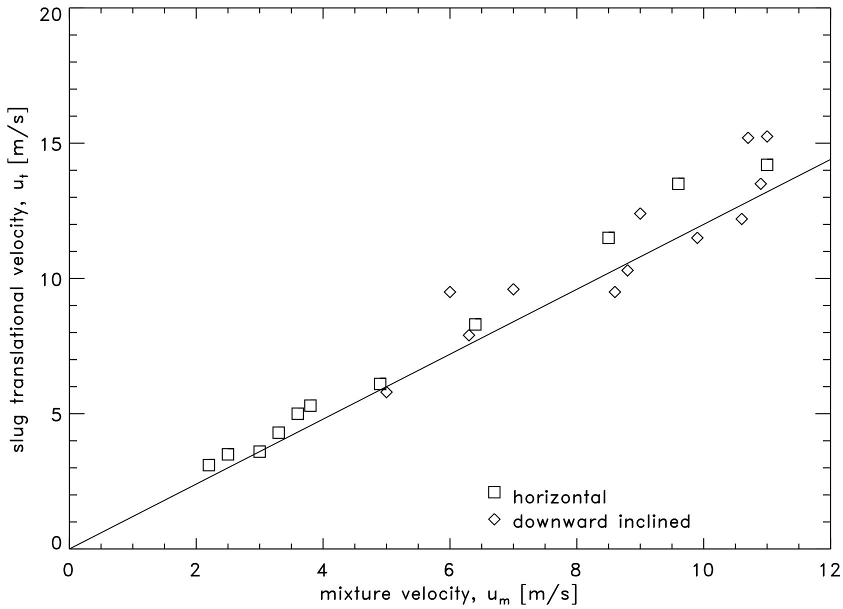

Fig. 16. Slug translational velocity in horizontal and downward pipes.

The computed and experimental mean liquid hold-ups are shown in Fig. 17. Here, the scatter in results is wider than those for slug frequency indicating a larger discrepancy between theory and experiment. This could be attributed to the neglect of gas entrainment into the body of the liquid

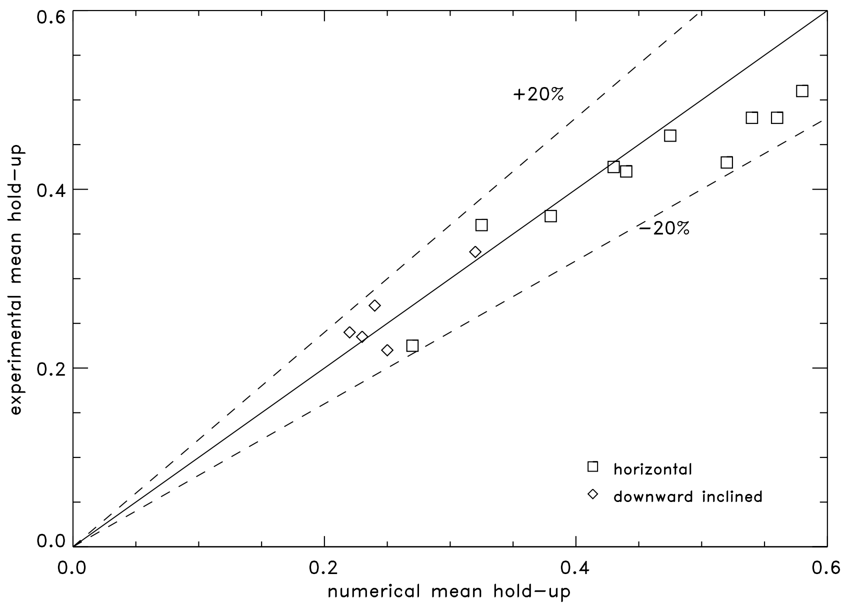

Fig. 17. Mean hold-up in horizontal and downward pipes.

slug in the present model, which would obviously affect the predicted hold-up. Account of the entrainment process is underway and is described by Bonizzi et al. (2001).

4.3. V-section

This case is an example where terrain slugging supplements and interacts with that due to hydrodynamic instabilities, often resulting in much longer slugs than in horizontal pipelines. At a V-section, liquid accumulates from the incoming and outgoing pipes, thereby changing the characteristics of incoming slugs. The configuration studied is shown in Fig. 8, which shows a 37 m V-section consisting of a downhill pipe of 14 m, and an uphill pipe of 23 m in length. Both sections are inclined at 1.5° to the horizontal.

The model captures the expected flow behaviour through this V-section dip. At low to moderate mixture velocities, stratified flow occurs in the downward sloping pipe, while slugs are generated in the upward sloping section. Slugging occurs in both sections at high mixture velocities.

In what follows, numerical predictions for low, moderate, and high mixture velocities are compared with available experimental data from the WASP facilities (Hale, 1999). The values of superficial gas and liquid velocities for the three cases are 6/0.6, 8/0.8, 10/1.0 m/s, respectively. Fig. 18 shows the slug frequency as a function of the mixture velocity; both, the experimental data and the numerical results show a similar trend of increasing slug frequency with increasing mixture velocity. The numerical results are within 30% of the experimental data.

The mean hold-up predictions are compared with experimental data in Fig. 19. Unlike the experimental data which show a decline, the mean predicted hold-up increases with the mixture

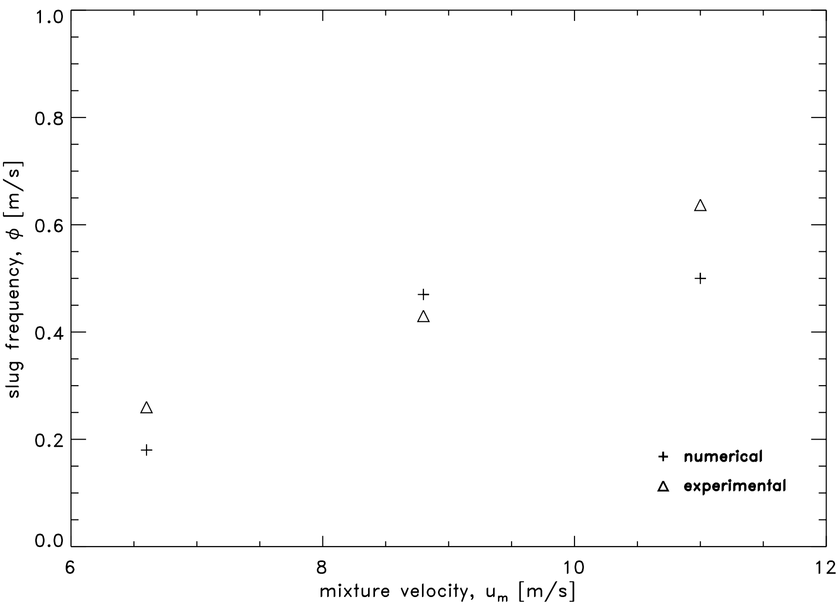

Fig. 18. Slug frequency in V-section pipe.

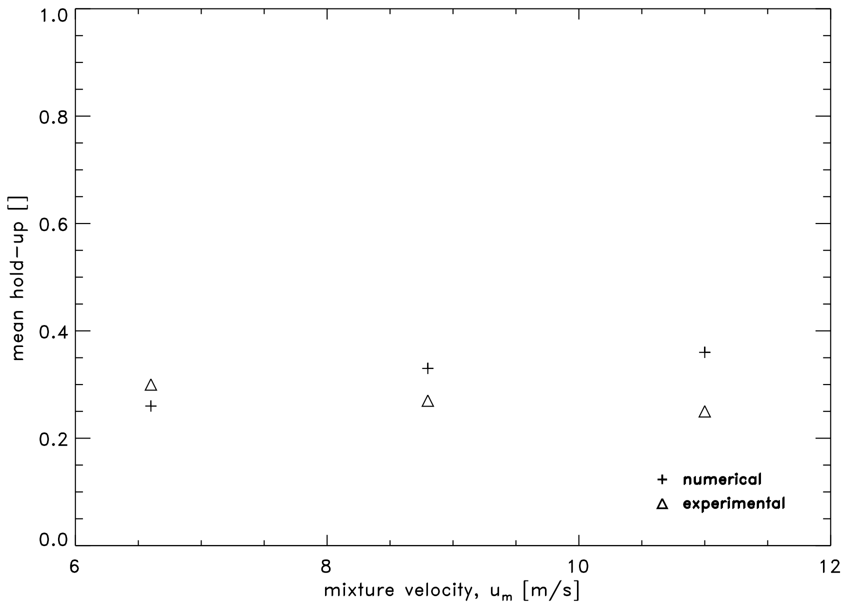

Fig. 19. Mean hold-up in V-section pipe.

velocity. The discrepancies are thought to be due to the neglect of gas entrainment into the liquid slug in the present study. Nonetheless, the first two hold-up cases are within 22% of the experimental data, with only case 3 showing a discrepancy of 44%. This level of variance between

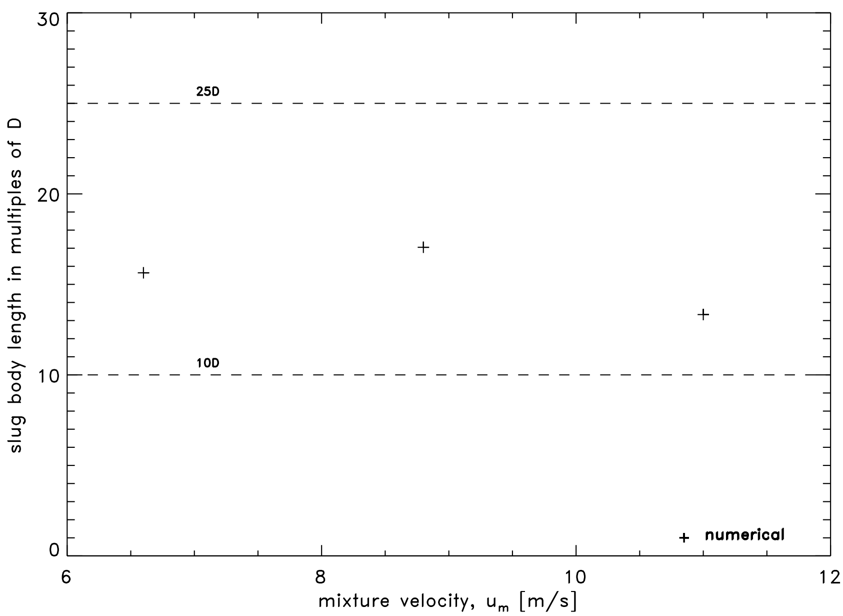

Fig. 20. Average slug body length in V-section pipe.

measurement and theory is quite reasonable given the uncertainties in the experiment, the complexity of the phenomenon modelled and the neglect of gas entrainment in the predictions.

Fig. 20 presents the computed slug body length for the three different mixture velocities. A typical range of the experimentally measured slug body length in horizontal and near horizontal pipe flow is between 10 and 25 pipe diameters (Dukler and Hubbard, 1975; Dukler et al., 1985; Nydal et al., 1992). The numerical calculations are well within the scattered data.

5. Conclusions

It has been demonstrated that the standard one-dimensional transient two-fluid model is able to simulate correctly the growth of instabilities in stratified flow, and to capture automatically their subsequent development into slugs. The simulated growth rate of instabilities compares well with analytic solutions obtained from linear stability analyses. The transition from stratified to slug flow is predicted to be close to what has been measured experimentally and to the widely accepted boundaries drawn by Taitel and Dukler. Furthermore, when slugs develop to form a fully intermittent slug flow, the slug characteristics such as slug length and frequency, are predicted quite well in comparison to the available data. This has been amply demonstrated by carrying out numerous computations for horizontal, slightly inclined and V-section pipes.

The accuracy of the simulations were shown to be sensitive to some of the closure models used to describe the shear forces in the momentum equations, and in particular the wall shear force on the liquid phase. For the latter, it was found that the Hand correlation for the friction factor gave the best overall results.

An important aspect in any numerical simulation is numerical accuracy. In the present work this was ensured by the use of fine enough meshes to yield grid-independent solutions. Failure to achieve this would lead to suppression of the growth of instabilities. This could result in either obtaining solutions to an ill-posed system of equations that might look plausible, but are non-physical, or to the prevention of the legitimate growth of waves to form slugs, when the equation system is well-posed.

Acknowledgements

This work has been undertaken within the Transient Multiphase Flow Coordinated Research Project. The authors wish to acknowledge the contributions made to this project by the Engineering and Physical Sciences Research Council (EPSRC) and to the following industrial organisations: ABB; AEA Technology; Amerada Hess; BG International; BP Amoco Exploration; CALtec; Chevron; Conoco; Granherne; Exxon Production Research; Institutt for Energiteknikk; Institut Francais du Petrole; Marathon Oil; Mobil North Sea; Norsk Hydro; Scandpower; Texaco Britain; TotalFinaElf. The authors wish to express their sincere gratitude for this support.

The authors also acknowledge the background work of C. Hale, and P.J. Wood-burn, and the numerous computer simulations of J. Rippiner, and M. Bonizzi. Thanks are extended to G.F. Hewitt and his team for the provision of experimental data and for the numerous discussions on the physics of the slug flow.

References

Agrawal, S.S., Gregory, G.A., Govier, G.W., 1973. An analysis of horizontal stratified two-phase flow in pipes. Can. J. Chem. Eng. 51, 280–286.

Anderson, J.D., 1995. Computational Fluid Dynamics. In: Mechanical Engineering Series. McGraw-Hill, New York.

Andreussi, P., Bendiksen, K., Nydal, O.J., 1993. Void distribution in slug flow. Int. J. Multiphase Flow 19, 817–828.

Andreussi, P., Persen, L.N., 1987. Stratified gas–liquid flow in downwardly inclined pipes. Int. J. Multiphase Flow 13, 565–575.

Andritsos, N., Hanratty, T.J., 1987. Influence of interfacial waves in stratified gas–liquid flows. AIChE J. 33, 444–454.

Ansari, M.R., 1998. Dynamical behavior of slug initiation generated by short waves in two-phase air–water stratified flow. ASME HTD 361, 289–295.

Barnea, D., 1991. On the effect of viscosity on stability of stratified gas–liquid flow—application to flow pattern transition at various pipe inclinations. Chem. Eng. Sci. 46, 2123–2131.

Barnea, D., Shoham, O., Taitel, Y., Dukler, A.E., 1980. Flow pattern transition for gas–liquid flow in horizontal and inclined pipes. Int. J. Multiphase Flow 6, 217–225.

Barnea, D., Taitel, Y., 1993. A model for slug length distribution in gas–liquid slug flow. Int. J. Multiphase Flow 19, 829–838.

Barnea, D., Taitel, Y., 1994. Interfacial and structural stability of separated flow. Int. J. Multiphase Flow 20, 387–414.

Bendiksen, K.H., Espedal, M., 1992. Onset of slugging in horizontal gas–liquid pipe flow. Int. J. Multiphase Flow 18, 237–247.

Bendiksen, K.H., Brandt, I., Jacobsen, K.A., Pauchon, C., 1987. Dynamic simulation of multiphase transportation systems. In: Multiphase Flow Technology and Conseqences for Field Development Forum, Stavanger, Norway.

Bendiksen, K.H., Malnes, D., Straume, T., Hedne, 1990. A non-diffusive numerical model for transient simulation of oil–gas transportation systems. In: Euro Sim. Multiconf., Nüremberg, 10–13 June.

Bendiksen, K.H., Malnes, D., Moe, R., Nuland, S., 1991. The dynamic two-fluid model OLGA: theory and application. SPE Prod. Eng. 6, 171–180.

Bendiksen, K.H., Malnes, D., Nydal, O.J., 1996. On the modelling of slug flow. Chem. Eng. Commun. 141–142, 71–102.

Black, P.S., Daniels, L.C., Hoyle, N.C., Jepson, W.P., 1990. Studying transient multiphase flow using the pipeline analysis code (PLAC). J. Energy Resour. Technol. 112, 25–29.

Bonizzi, M., 2002. Transient one-dimensional modelling of multi-phase slug flows. Ph.D. Thesis, Imperial College, University of London.

Bonizzi, M., Issa, R.I., Kempf, M.H.W., 2001. Modelling of gas entrainment in horizontal slug flow. In: International Conference on Multiphase Flow, New Orleans, USA.

Bouré, J., Réocreux, M., 1972. General equations of two-phase flows. In: All Union Heat Mass Transfer Conference, Minsk, USSR.

Brauner, N., Maron, M.D., 1992. Stability analysis of stratified liquid–liquid flow. Int. J. Multiphase Flow 18, 103–121.

De Henau, V., Raithby, G.D., 1995a. A transient two-fluid model for the simulation of slug flow in pipelines: I. Theory. Int. J. Multiphase Flow 21, 335–349.

De Henau, V., Raithby, G.D., 1995b. A transient two-fluid model for the simulation of slug flow in pipelines: II. Validation. Int. J. Multiphase Flow 21, 351–363.

Dukler, A.E., Fabre, J., 1992. Gas–liquid slug flow-knots and loose ends. in: 3rd International Workshop Two-Phase Flow Fundamentals, Imperial College.

Dukler, A.E., Hubbard, M.G., 1975. A model for gas–liquid slug flow in horizontal and near horizontal tubes. Ind. Eng. Chem. Fund. 14, 337–345.

Dukler, A.E., maron, D., Brauner, N., 1985. A physical model for predicting the minimum stable slug length. Chem. Eng. Sci. 40, 1379–1385.

Drew, D.A., 1983. Mathematical modeling of two-phase flow. Ann. Rev. Fluid. Mech. 15, 261–291.

Espedal, M., Bendiksen, K.H., 1989. Onset of instabilities and slugging in horizontal and near-horizontal gas–liquid flow. European Two-Phase Flow Group Meeting, Paris, May 9–June 1, paper G4, pp. 1–30.

Fabre, J., Liné, A., 1992. Modeling of two-phase slug flow. Ann. Rev. Fluid Mech. 24, 21–46.

Fabre, J., Ferschneider, G., Masbernat, L., 1983. Intermittent gas liquid flow modelling in horizontal or weakly inclined pipes. In: International Conference on Physical Modellling for Multiphase Flow, Coventry, pp. 233–254.
Fabre, J., Liné, A., Peresson, L., 1992. Two fluid/two flow pattern model for transient gas liquid flow in pipes. In: 4th International Conference on Multiphase Flow, Nice, pp. 269–284.
Fagundes Netto, J.R., Fabre, J., Peresson, N.L., 1999. Shape of long bubbles in horizontal slug flow. Int. J. Multiphase Flow 25, 1129–1160.
Fan, Z., Lusseyran, F., Hanratty, T.J., 1993a. Initiation of slugs in horizontal gas–liquid flows. AIChE J. 39, 1741–1753.
Fan, Z., Ruder, Z., Hanratty, T.J., 1993b. Pressure profiles for slugs in horizontal pipes. Int. J. Multiphase Flow 19, 421–437.
Ferschneider, G., 1983. Ecoulements gaz–liquide à poches et à bouchons en conduite. Rev. Inst. Fr. Pét. 38, 153–182.
Garabedian, P.R., 1964. Partial Differential Equations. John Wiley, New York.
Gomez, L.E., Shoham, O., Schmidt, Z., Chokshi, R.N., Brown, A., Northug, T., 1999. A unified mechanistic model for steady-state two-phase flow in wellbores and pipelines. In: SPE Annual Technological Conference Exhibition, Houston, Texas, USA, SPE 56520, pp. 307–320.
Gregory, G.A., Scott, D.S., 1969. Correlation of liquid slug velocity and frequency in horizontal cocurrent gas–liquid slug flow. AIChE J. 15, 935–993.
Grolman, E., Commandeur, N., De Baat, E., Fortuin, J., 1996. Wavy to slug flow transition in slightly inclined gas–liquid pipe flow. AIChE J. 42, 901–907.
Grolman, E., Fortuin, J.H., 1996. Waves and instabilities in inclined gas–liquid pipe flow. ASME HTD 334, 163–170.
Hale, C.P., 1999. Slug flow in a V-section. Private communications. Chemical Engineering Department, Imperial College.
Hand, N.P., 1991. Gas–liquid co-current flow in a horizontal pipe. Ph.D. Thesis, Queen's University Belfast.
Ishii, M., 1975. Thermo-Fluid Dynamic Theory of Two-Phase Flow. Eyrolles, Paris.
Ishii, M., Mishima, K., 1984. Two-fluid model and hydrodynamic constitutive relations. Nucl. Eng. Des., 107–126.
Issa, R.I., Abrishami, Y., 1986. Computer modelling of slugging flow. Technical Report, Mechanical Engineering Department, Imperial College.
Issa, R.I., Woodburn, P., 1998. Numerical prediction of instabilities and slug formation in horizontal two-phase flows. In: 3rd International Conference on Multiphase Flow, ICMF98, Lyon, France.
Jansen, F.E., Shoham, O., Taitel, Y., 1996. The elemination of severe slugging. Int. J. Multiphase Flow 22, 1055–1072.
Jepson, W.P., 1989. Modelling the transition to slug flow in a horizontal conduit. Can. J. Chem. Eng. 67, 731–740.
Jones, V., Prosperetti, A., 1985. On the suitability of first-order differential models for two-phase flow prediction. Int. J. Multiphase Flow 11, 133–148.
Kordyban, E.S., Ranov, T., 1970. Mechanism of slug formation in horizontal tubes. J. Basic Eng. TASME, 857–864.
Kowalski, J.E., 1987. Wall and interfacial shear stress in stratified flow in a horizontal pipe. AIChE J. 33, 274–281.
Lin, P.Y., Hanratty, T.J., 1986. Prediction of the initiation of slugs with linear stability theory. Int. J. Multiphase Flow 12, 79–98.
Liné, A., 1983. Ecoulement intermittent de gaz et de liquide en conduite verticale. Thèse Institute Nationale Polytechnique, Toulouse.
Lunde, O., Asheim, H., 1989. An experimental study of slug stability in horizontal flow. In: 4th International Multiphase Flow Conference, Nice, France, 19–21 June, pp. 419–430.
Manolis, I.G., 1995. High pressure gas–liquid slug flow. Ph.D. Thesis, Imperial College.
Manolis, I.G., Mendes-tatsis, M.A., Hewitt, G.F., 1995a. The effect of pressure on flow pattern transition and pressure gradient in two-phase horizontal slug. In: IChemE Research Event, Edinburgh, UK, 5–6 January.
Manolis, I.G., Mendes-Tatsis, M.A., Hewitt, G.F., 1995b. The effect of pressure on slug frequency in two-phase horizontal flow. In: 2nd International Multiphase Flow Conference, Kyoto, Japan, 3–7 April.
Mishima, K., Ishii, M., 1986. Theoretical prediction of onset of horizontal slug flow. J. Fluids Eng. 102, 441–444.
Moissis, R., Griffith, P., 1962. Entrance effects in two-phase slug flow. J. Heat Transfer 84, 29–39.
Nydal, O.J., Banerjee, S., 1996. Dynamic slug tracking simulations for gas–liquid flow in pipelines. Chem. Eng. Commun. 141–142, 13–39.

Nydal, O.J., Pintus, S., Andreussi, P., 1992. Statistical characterization of slug flow in horizontal pipes. Int. J. Multiphase Flow 18, 439–453.

Nydal, O.J., Andreussi, P., 1991. Gas entrainment in a long liquid slug advancing in a near horizontal pipe. Int. J. Multiphase Flow 17, 179–189.

Ruder, Z., Hanratty, P.J., Hanratty, T.J., 1989. Necessary conditions for the existence of stable slugs. Int. J. Multiphase Flow 15, 209–226.

Schmidt, Z., Doty, D.R., Dutta-Roy, K., 1985. Severe slugging in offshore pipeline riser-pipe systems. Soc. Pet. Eng. J., 27–38.

Song, J.H., Ishii, M., 2000. The well-posedness of incompressible one-dimensional two-fluid model. Int. J. Heat Mass Transfer 43, 2221–2231.

Spedding, P.L., Hand, N.P., 1997. Prediction in stratified gas–liquid co-current flow in horizontal pipelines. Int. J. Heat Mass Transfer 40, 1923–1935.

Srichai, S., 1994. High pressure separated two-phase flow. Ph.D. Thesis, Imperial College.

Stanislav, J.F., Kokal, S., Nicholson, M.K., 1986. Intermittent gas–liquid flow in upward inclined pipes. Int. J. Multiphase Flow 12, 325–335.

Straume, T., Nordsveen, M., Bendiksen, K., 1992. Numerical simulation of slugging i pipelines. Multiphase Flow Wells Pipelines, 144.

Stuhmiller, J.H., 1977. The influence of interfacial pressure forces on the character of two-phase flow equations. Int. J. Multiphase Flow 3, 551–560.

Taitel, Y., Barnea, D., 1990. Two-phase slug flow. Adv. Heat Transfer 20, 83–132.

Taitel, Y., Barnea, D., 1998. Effect of gas compressibility on a slug tracking model. Chem. Eng. Sci. 53, 2089–2097.

Taitel, Y., Dukler, A.E., 1976. A model for predicting flow regime transitions in horizontal and near horizontal gas–liquid flow. AIChE J. 22, 47–55.

Taitel, Y., Sarica, C., Brill, J.P., 2000. Slug flow modelling for downward inclined pipe flow: theoretical considerations. Int. J. Multiphase Flow 26, 833–844.

Vernier, P., Delhaye, J., 1968. General two-phase flow equations applied to the thermodynamics of boiling nuclear reactors. Energ. Primarie 4, 1–43.

Wallis, G.B., 1969. One-dimensional Two-phase Flow. McGraw-Hill, New York.

Watson, M., 1989. Wavy stratified flow and the transition to slug flow. In: 4th International Multiphase Flow Conference, Nice, France, 19–21 June, paper G3.

Woodburn, P.J., Issa, R.J., 1998. Well-posedness of one-dimensional transient, two-fluid models of two-phase flows. In: 3rd International Symposium on Mulitphase Flow, ASME Fluids Engineering Division Summer Meeting, Washington, USA.

Woods, B.D., Hurlburt, E.T., Hanratty, T.J., 2000. Mechanism of slug formation in downwardly inclined pipes. Int. J. Multiphase Flow 26, 977–998.

Zheng, G., Brill, J.P., Taitel, Y., 1994. Slug flow behavior in a hilly terrain pipeline. Int. J. Multiphase Flow 20, 63–79.